Automated Ultrasound Scanning on a Dual-Modality Breast Imaging System

Coverage and Motion Issues and Solutions

Sumedha P. Sinha, MS, Mitchell M. Goodsitt, PhD, Marilyn A. Roubidoux, MD, Rebecca C. Booi, MS, Gerald L. LeCarpentier, PhD, Christine R. Lashbrook, RT(R)(M), Kai E. Thomenius, PhD, Carl L. Chalek, PhD, Paul L. Carson, PhD

Objective. We are developing an automated ultrasound imaging-mammography system wherein a digital mammography unit has been augmented with a motorized ultrasound transducer carriage above a special compression paddle. Challenges of this system are acquiring complete coverage of the breast and minimizing motion. We assessed these problems and investigated methods to increase coverage and stabilize the compressed breast. ***Methods.*** Visual tracings of the breast-to-paddle contact area and breast periphery were made for 10 patients to estimate coverage area. Various motion artifacts were evaluated in 6 patients. Nine materials were tested for coupling the paddle to the breast. Fourteen substances were tested for coupling the transducer to the paddle in lateral-to-medial and medial-to-lateral views and filling the gap between the peripheral breast and paddle. In-house image registration software was used to register adjacent ultrasound sweeps. ***Results.*** The average breast contact area was 56%. The average percentage of the peripheral air gap filled with ultrasound gel was 61%. Shallow patient breathing proved equivalent to breath holding, whereas speech and sudden breathing caused unacceptable artifacts. An adhesive spray that preserves image quality was found to be best for coupling the breast to the paddle and minimizing motion. A highly viscous ultrasound gel proved most effective for coupling the transducer to the paddle for lateral-to-medial and medial-to-lateral views and for edge fill-in. ***Conclusions.*** The challenges of automated ultrasound scanning in a multimodality breast imaging system have been addressed by developing methods to fill in peripheral gaps, minimize patient motion, and register and reconstruct multisweep ultrasound image volumes. ***Key words:*** acoustic coupling; automated breast ultrasound scanning; breast cancer screening; complete coverage; motion artifacts.

This study was part of a project aimed at improving the efficacy of breast cancer diagnosis and characterization by acquiring images of the breast in the same geometry with x rays and ultrasound.[1–3] The automated ultrasound imaging is acquired though a special compression paddle[4] that is also used for x-ray imaging. Possible ultrasound modes are 3-dimensional (3D) ultrasound imaging in gray scale (B-mode), Doppler color flow imaging, elasticity imaging, and compounding. This report focuses on gray scale ultrasound imaging, with additional results obtained from elasticity imaging.

X-ray and ultrasound images can be acquired with the dual-modality system in the conventional mammography views: craniocaudal (CC), medial-lateral-oblique, lateral-medial-oblique, lateral-to-medial (LM), and medial-to-

lateral (ML). The ultrasound transducer is placed in a holder that is attached to an x-y translator drive, which moves the transducer across the compression paddle under computer control. One to 3 adjacent automated ultrasound transducer sweeps are performed as needed for the area of coverage, depending on the shape and size of the patient's breast. The 3D ultrasound images obtained are later registered and fused to visualize the entire breast volume. Fusion requires a high degree of accuracy. The final image volume is usually evaluated[5] in conjunction with a 3D mammogram[6] (tomosynthesis). Two approaches to achieve adjacent sweep alignment are stabilizing the breast while in compression and post processing (ie, shifting, tilting, and warping) the obtained images.

A major problem associated with performing ultrasound scans through a compression paddle is that there can be an appreciable air gap between the paddle and the breast surface near the breast periphery. This gap is illustrated in Figure 1.

Because ultrasound is highly reflected at the paddle/air interface, and very little ultrasound at diagnostic imaging frequencies transmits through air, any region of the breast where there is such an air gap will not be visible in the ultrasound image. Our purpose was to investigate the magnitude of the ultrasound coverage problem and possible solutions.

Figure 1. Breast-simulating phantom illustrating an air gap between the phantom and the compression paddle at the periphery.
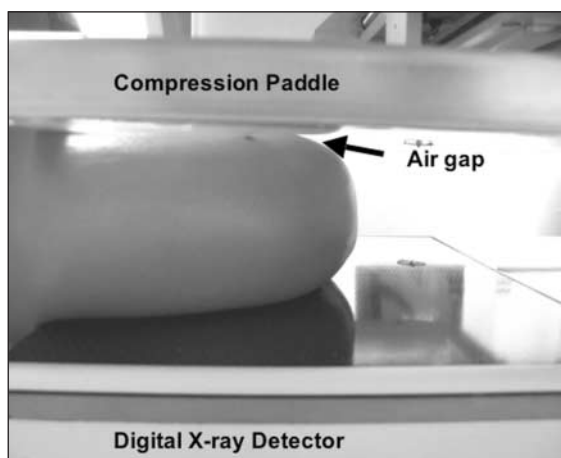
An additional issue is how to minimize breast motion and yet provide coupling of the breast to the compression paddle. Traditional ultrasound gels exhibit excellent ultrasound transmission properties but are too slippery for maintaining the breast in a fixed position in contact with the paddle throughout scan times that can last several minutes. In addition, patient motion due to breathing and speaking can create artifacts that distort the gray scale ultrasound image. Furthermore, breast slippage is undesirable for elasticity imaging, which may be implemented after the automated ultrasound sweeps are obtained by further compressing the human patient's breast in small increments up to an additional 5% strain. Digitized radio frequency signals acquired for elasticity studies are later correlated, and displacement estimates are converted to strain images. Although elasticity imaging has proven to be a valuable diagnostic tool, like image fusion, it is very sensitive to breathing motion. We quantified 4 different motion artifacts for B-mode and in phase/quadrature phase (IQ) radio frequency data and explored methods to minimize such artifacts.

Materials and Methods

Institutional Review Board approval was obtained for this study (2002-0584, University of Michigan), and informed consent was obtained for every patient in these trials. Initially, testing was done on a first-generation dual-modality ultrasound/digital mammography system consisting of a GE LOGIQ 9 ultrasound system (GE Healthcare, Milwaukee, WI) and a GE Senographe 2000D digital mammography unit. Subsequent testing was performed on a combined system consisting of a LOGIQ 9 ultrasound system and a second-generation GE Global Research tomosynthesis unit.[7] The ultrasound transducer used was a GE M12L linear matrix array operating at maximum center frequencies of 10 to 12 MHz. The ultrasound system was augmented with a motorized transducer carriage that translated the transducer from left to right over a water-filled or gel-filled 4-methylpentene-1-based polyolefin (TPX) plastic compression paddle of 2.5 mm in thickness (Figure 2). Water was used as a coupling agent between the transducer and the pad-

dle for CC views, and gel was used for oblique and lateral views. Software developed by GE Global Research was used to drive the motorized carriage.

The compression paddle is a device used to compress the breast in mammography, in which compression reduces image degradation due to motion, x-ray scatter, and x-ray beam hardening and lowers the required radiation dose. Inasmuch as a longer duration of compression is necessary for automated ultrasound scanning, a compression force of about 4 to 10 dN is typically used with the dual-modality system to minimize patient discomfort while stabilizing the breast.

Estimation of Coverage

To estimate the fraction of the breast surface area that was in contact with the compression paddle, technologists made visual tracings of the paddle-to-breast contact region and the outer breast border on transparencies placed on the compression paddle. These tracings were drawn for 10 patients (7 with known breast cancer and 3 healthy volunteers). The tracings were then digitized with a flatbed scanner and analyzed with ImageJ, a public domain Java image-processing program inspired by NIH Image (http://rsb.info.nih.gov/ij/docs/intro.html), to measure the contact and total breast surface areas and the

linear dimensions of the peripheral air gaps. To fill in the air gap between the breast and the compression paddle at the curvature of the breast periphery, we developed a technique using a syringe to dispense bubble-free gel at this location. The linear dimensions of the gap filled with ultrasound gel were estimated from ultrasound images of 10 different volunteers.

Couplant Selection

Couplant Between Breast and Compression Paddle
To test agents for coupling the breast to the paddle, various adhesives were qualitatively assessed for the absence of coupling gaps and shear/slippage resistance. The tests were carried out on a human wrist. The compression paddle was in the CC position and was filled with water for coupling the transducer to the paddle. The couplant candidates were then each applied to the wrist, and the wrist was lightly compressed with the paddle. Gray scale ultrasound images were then acquired of the same area of the wrist. The adhesive couplant candidates that were tested included Got2b Glued hair spray (Schwarzkopf & Henkel, Irvine, CA), Giga Hold hair spray (Continental Consumer Products, Birmingham, MI), Skintac adhesive (Torbot Group Inc, Cranston, RI), SonTac gel pads (Diagnostic Ultrasound Corporation, Bothell,

Figure 2. A, Close-up of automated scanning equipment. **B**, Schematic illustrating relative positions of the breast, x-ray detector, transducer, compression paddle, and couplants. (The thickness of the adhesive couplant is exaggerated for improved visibility.)

A
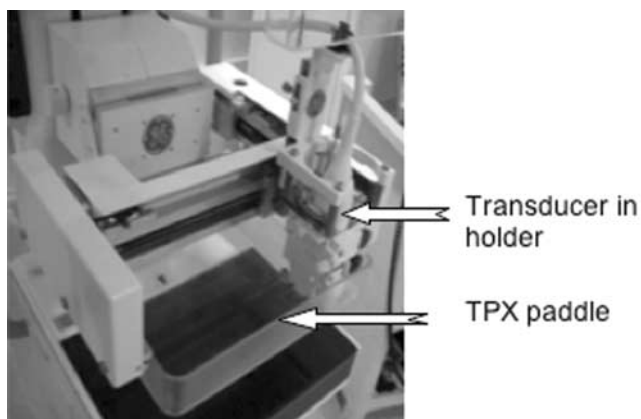
B
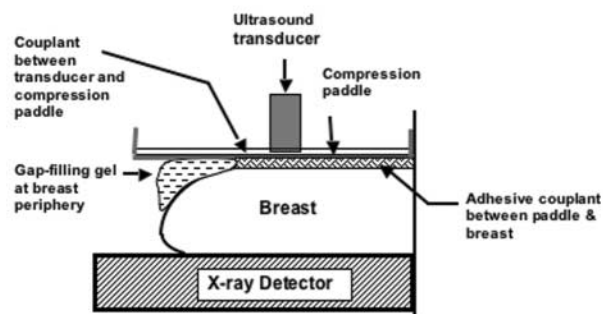
WA), shaped Gel Concepts pads (Gel Concepts, Whippany, NJ), Tensive glue (Parker Laboratories, Fairfield, NJ), YES! paste (Gane Brothers and Lane, Elk Grove Village, IL), Got2b Glued spiking glue (Schwarzkopf & Henkel), and PoliGrip dental paste (GlaxoSmithKline, Moon Township, PA). Aquasonic gel (Parker Laboratories), a conventional ultrasound coupling gel, was used as a reference standard for comparisons. In addition to the absence of gaps and good shear/slippage resistance, we also qualitatively evaluated image quality, ease of use, and aftereffects, if any.

Next, these agents were quantitatively assessed by measuring the contrast-to-noise ratios (CNRs) in images of the 2.4-mm-diameter anechoic and –9-dB cylindrical targets within a Computerized Imaging Reference Systems (CIRS) model 047 gray scale contrast detail ultrasound phantom (Computerized Imaging Reference Systems, Inc, Norfolk, VA). Cross-sectional B-mode images of these targets were taken at different depths (namely, 2.5 and 4 cm) with and without an intervening 2.5-mm-thick piece of TPX plastic. The TPX plate was a smaller version of the compression paddle that was more convenient to use when imaging the phantom. The coupling agents were placed between the TPX and the phantom scanning window. The resulting images were then analyzed to compute the CNRs within selected targets in the phantom.

The CNR was evaluated[8] as

$$CNR = (\mu_t - \mu_b)/\sigma_{rms},$$

where μ_t was the mean signal level in the target region of interest (ROI); μ_b was the mean signal level in the background ROI; and σ_{rms} was the root mean square noise in the background. μ_b and σ_{rms} were obtained as the average of mean and SD values in 6 background ROIs in the phantom at the same depth as the targets.

We also obtained comparable images of a cyst in a patient's breast using Got2b Glued (the most viable coupling agent from our qualitative and quantitative results) and LithoClear ultrasound gel (Sonotech, Bellingham, WA). The CNRs for the cyst were evaluated by the formula above, picking 6 background ROIs all around the periphery of the cyst.

Couplant Between Transducer and Compression Paddle in ML and LM Views

For coupling the transducer to the paddle in the LM and ML views, various gels, lotions, and oils were qualitatively assessed for viscosity. These were Sonotech LithoClear gel, Sonotech Clear Image gel (both low- and high-viscosity types), Medichoice gel (Owens and Minor, Richmond, VA), Polysonic lotion (Parker Laboratories), Parker Aquasonic gel, General Imaging gel (ATL, Reedsville, PA), Primrose oil (Cedar Vale Natural Health, Cedar Vale, KS), Nutra-E oil (Nature Made Nutritional Products, Los Angeles, CA), glycerin, and 3 mixtures of Polysonic gel with LithoClear gel (ratios, 1:2, 1:1, and 2:1). The parameters for this test were gel movement after 3 and 6 minutes for a given layer thickness.

Motion Analysis

Ultrasound image data were collected in the B-mode and IQ mode for analysis of artifacts caused by patient motion during scans. Automated full-coverage ultrasound scanning was carried out in the B-mode, whereas IQ data were collected (also in the automated mode) during elasticity data acquisitions. Six (7 for elasticity) patient volunteers were asked to do the following during short stationary scans: (1) hold their breath; (2) take a deep breath and release it; (3) breathe shallowly; and (4) talk (repetition of a single phrase). Every image was split into 8 regions, and each of these regions was correlated individually across successive image frames at the pixel level. The minimum observed correlation was noted for each region. Elasticity data were correlated at the subpixel level over the whole image, and average correlation was noted. Furthermore, the correlation maintained in successive image frames was checked over time for a stationary scan. This was done to quantify the maintenance of adhesive properties over time.

To best splice adjacent ultrasound sweep images into a 3D volume, it is advisable to include redundant data in the form of an overlap between sweeps. The automated ultrasound scanning system was programmed to scan the breast with an overlap of 1 cm between adjacent sweeps. The actual overlap could be different because of factors such as possible bowing of the

compression paddle and looseness of the transducer holder. The true overlaps or shifts were determined using the Miami Fuse[9] registration application.

Results

Estimation of Coverage

Examples of the visual traces of the breast-paddle contact areas and breast outer boundaries are shown in Figure 3. The percentages of the breast area in contact with the compression paddle from the visual tracings without gel are listed in Table 1.

The percentages of the breast area in contact with the paddle ranged from 35% (Figure 3A) to 74% (Figure 3B) with a mean ± SD of 56% ± 15%. The linear dimensions of the gaps between the border of the contact region and the outer border of the breast in the tracings are listed in Table 2. These gaps were measured at 4 different angles relative to the approximate centers of the breasts at the chest wall (Figure 3). For these 10 patients, the gap dimensions ranged from 0.8 to 4.3 cm with a mean of 2.2 ± 0.9 cm.

Analysis of the B-mode ultrasound images obtained with the automated system on 10 different volunteers who were subsequently scanned with the gaps filled in with gel indicated that had gel not been used, air gaps would have ranged between 0.7 and 4.7 cm (mean, 1.7 ± 0.6 cm). The analysis also indicated that the percentages of the linear dimensions of the gaps that

were filled in with gel ranged from 42% to 85% with a mean of 61% ± 10%.

Figure 4 is a B-mode single slice from a 3D ultrasound volume showing how gel fill-in improves breast coverage. Most of the breast beneath the gel-filled region shown in this figure would not have been imaged without the gel.

Couplant Selection

Our qualitative comparison indicated that the most suitable coupling agent between the breast and the compression paddle was the water-soluble hair spray Got2b Glued. Another water-soluble hair spray, Giga Hold, and a liquid adhesive that is used to attach ostomy and other appliances to skin, Skintac, also performed well. The latter, however, is not water soluble and must be removed with alcohol.

When various viscous substances were qualitatively tested for coupling the transducer to the compression paddle in the lateral view, Sonotech LithoClear gel performed best overall. This was also the gel chosen for filling in the gap at the periphery of the breast.

Figures 5 and 6 compare the relative image quality obtained with the automated ultrasound scanning system using Got2b Glued hair spray and LithoClear ultrasound gel as the coupling media between the TPX paddle and the breast. Visual inspections of these patient images as well as quantitative measurement of a CNR improvement of 2.5% for the Got2b Glued couplant proved that the adhesive spray did not degrade

Figure 3. Visual tracings of regions of the breast in contact with the paddle (inner curves) and outer breast borders. **A**, The area of the breast in contact with the paddle is 28.7 cm², and the total breast area is 81.9 cm², yielding a minimum percentage of the breast area in contact with the paddle of 35%. **B**, The area of the breast in contact with the paddle is 80.2 cm², and the total breast area is 108 cm², yielding a maximum percentage area in contact with the paddle of 74%.
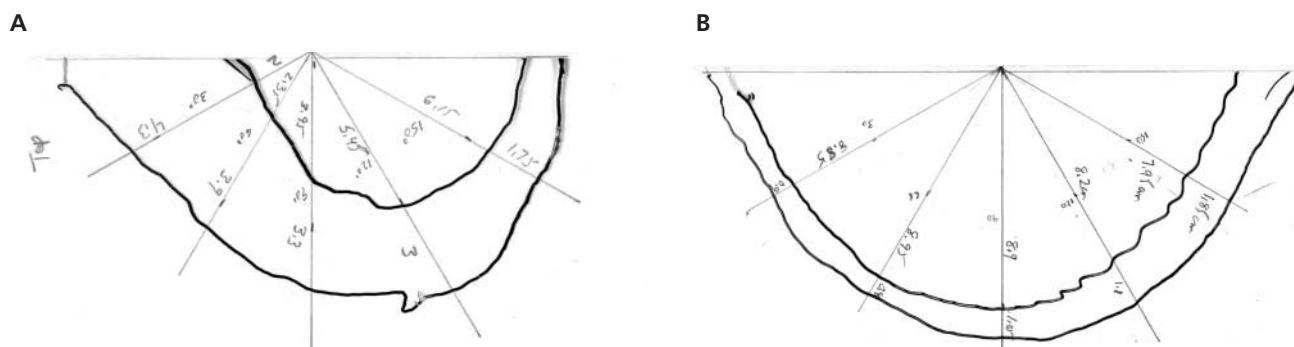
A

B

Table 1. Percentage of Breast Area in Contact With the Compression Paddle From Visual Tracings (No Gel)

Patient	Area in Contact With Paddle, cm^2	Total Breast Area, cm^2	Breast Area in Contact With Paddle, %
1	114.8	154.4	74.4
2	65.6	103.7	63.2
3	28.0	62.7	44.7
4	51.9	105.0	49.4
5	35.7	84.7	42.2
6	36.2	80.1	45.2
7	28.7	81.9	35.1
8	126.9	193.1	65.8
9	80.2	108.4	73.9
10	50.4	71.6	70.4

image quality compared with ultrasound gel. Also, it maintained the correlation over time. See Figure 7 for the B-mode correlation over 5 minutes, which is the average time during which the patient is in compression.

Figures 8 and 9 graphically represent CNR values obtained for the anechoic and –9-dB (2.4-mm diameter and 4.52-mm^2 cross-sectional area) targets in the CIRS gray scale phantom. Circular ROIs of 2 different sizes (55 pixels [0.92 mm^2] and 130 pixels [2.16 mm^2]) were analyzed in several identical test images, and the best results were selected in each case. The ROIs were positioned at the centers of the targets by eye. The smaller ROI provided information about image degradation in the middle of the targets due to the coupling agent and was related to potential decreases in target conspicuity. The larger ROI provided more generalized information about image degradation, in particular, fill-in due to the coupling agent. "Water without TPX" was the case in which water was used

Table 2. Linear Dimensions of the Gaps at the Breast Periphery From Visual Tracings (No Gel)

Patient	Noncontact Gaps at Breast Periphery, cm				
	30°	60°	90°	120°	150°
1	0.9	0.8	1.05	1.8	1.85
2	3.6	2.6	2.7	3.1	2
3	3.2	2.5	2.1	2.35	1.8
4	3.85	3.25	3.55	2.7	1.6
5	3.85	2.25	2.1	1.5	1.4
6	2	2.2	3.1	2.9	2.6
7	4.3	3.9	3.3	3	1.75
8	2.6	2.3	2.25	1.75	1.6
9	1.3	0.9	1.45	1	1.1
10	0.85	1	1.9	1.45	1.1

between the transducer and the phantom, without an intervening TPX paddle. "Water with TPX" was the reference standard case in which a 2.5-mm-thick piece of TPX (heretofore referred to as the "TPX plate") was inserted between the transducer and the phantom, and water was used as the coupling agent between the TPX plate and the phantom. All the other agents were tested with the TPX plate inserted. Aquasonic gel was used to couple the transducer to the paddle in all cases, and either water or the agents being tested were used to couple the paddle to the phantom. Of the 3 agents tested (Got2b Glued, Giga Hold, and Skintac), Skintac had the best CNR value in 6 of 8 cases.

Figures 10 and 11 show background mean and root mean square (RMS) noise values obtained in the CIRS gray scale phantom at the 2.5- and 4-cm depths, respectively, for both 55- and 130-pixel areas. In general, inserting the 2.5-mm-thick TPX plate between the transducer and the phantom with water as the coupling agent resulted in a decrease in the average background pixel value by 27.9% at a depth of 2.5 cm and 32.5% at a depth of 4 cm. There were small (<10%) additional losses in the average background pixel values for the adhesives with TPX compared to water with TPX. The RMS background noise was less for water with TPX compared with water without TPX, probably because of the smaller average pixel values when TPX was present. Finally, the RMS background noise for the adhesives with TPX was in most cases within about 10% of those for water with TPX.

Motion Analysis

Figures 12 and 13 graphically represent the results for B-mode analysis of motion artifacts. The mean and SD for each artifact are included in Table 3. In the graphs in Figures 12 and 13, the 4 bars represent the averages of the minimum correlation values (minimum obtained in the 8 areas analyzed in each image) observed for each of the 4 experimental techniques. The error bars represent ±1 SD.

In general (combining the data for both breasts), when a minimum correlation was observed for B-mode data at the pixel level, breath holding ($R = 0.97$) and shallow breathing ($R = 0.97$) caused the least decorrelation, whereas speech

caused an intermediate decorrelation ($R = 0.91$), and deep breathing caused the most ($R = 0.81$). Two-sample Wilcoxon test results over every pair of different artifact correlation results for the left and right breasts individually indicate that the 4 methods analyzed had statistically significant mean differences between them ($P \ll .05$). Wilcoxon tests comparing artifact correlations in patients' left breasts with those in patients' right breasts did not indicate a statistically significant mean difference between the left and right breasts ($P \gg .05$), except for breath holding.

These findings were similar to those obtained for elasticity imaging. When an average correlation was observed for IQ data at the subpixel level, shallow breathing caused the least decorrelation ($R = 0.96$), whereas breath holding also had a relatively high correlation value ($R = 0.93$). Speech caused an intermediate decorrelation ($R = 0.87$), and deep breathing caused the most ($R = 0.73$). Two-sample Wilcoxon test results indicated that shallow breathing, breath holding, and talking were statistically significantly different from deep breathing ($P \ll .05$) but not from each other ($P \gg .05$). Correlation differences for the same artifact between the left and right breasts were not statistically significantly different ($P \gg .05$).

Registration of shifted sweeps in Miami Fuse,[9,10] to splice them to form the complete 3D volume, resulted in a negligible overlap error of 0.55 to 0.65 mm. Figure 14 is an example of a recently spliced image volume in which 2 sweeps were trimmed and fused to complete the volume.

Discussion

Estimation of Coverage

The gaps between the breast and the compression paddle at the breast periphery can limit ultrasound coverage to only half of the total breast area for the combined x-ray/ultrasound imaging system. Filling the gaps with LithoClear ultrasound gel using a syringe is effective at solving this problem, reducing the gap lengths by about 60%. This solution is only partial because 73% of malignant lesions are present at the periphery of the breast, as defined by a zone 1 cm wide beneath the subcutaneous fat or anterior to the retromammary fat.[11] However, it is possible to

Figure 4. Single slice of a spliced gray scale image volume with gel fill-in around the breast border.

image the axillary tail and extreme medial regions of the breast better by using lateral views. The subareolar region can be imaged better by compressing the breast such that the nipple is closer to the TPX paddle, therefore reducing the gap between the paddle and the subareolar region.

Figure 5. Cyst in a patient's breast imaged through the compression paddle with Got2b Glued spray between the breast and the paddle. The patient had multiple cysts in both breasts.
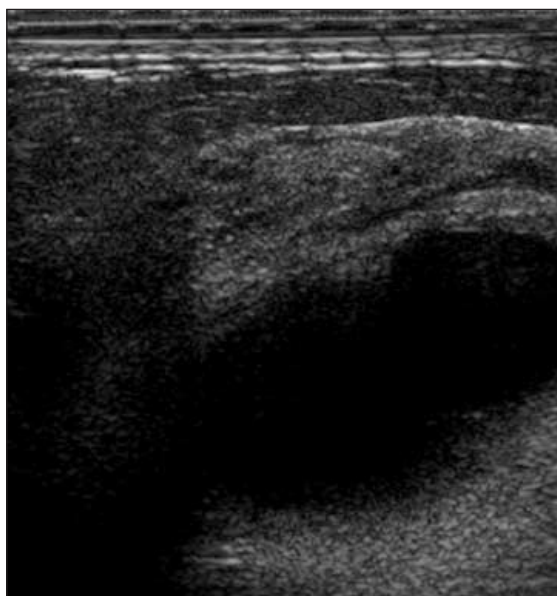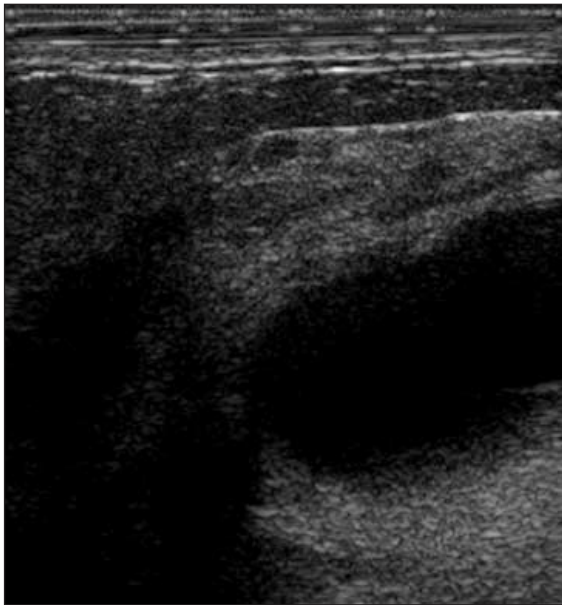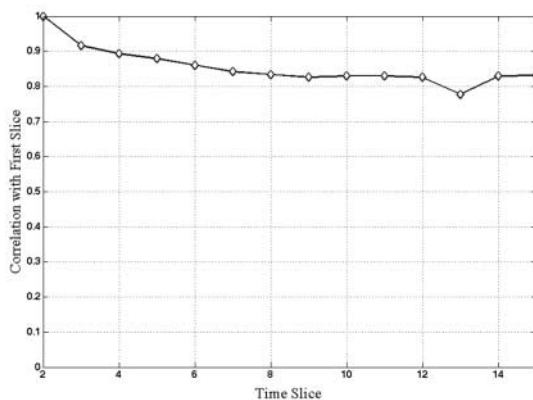
Figure 6. Same cyst as in Figure 5 imaged through the compression paddle with ultrasound gel between the breast and the paddle.

Couplant Selection

Nine different materials were tested for acoustic coupling of the compression paddle to the breast. Their coupling strengths, effects on image CNR, and practicability were compared, and the optimal substance was chosen. In all cases, water without the TPX layer produced the best CNR values. Water with the TPX layer showed better CNR values than the other agents in all cases except 1. The insertion of the TPX plate (paddle) was found to reduce the CNR value on the average by 11.3% at a depth of 2.5 cm and by 15.8% at a depth of 4 cm for gray scale images. It also reduced the average pixel value in the background region by 30.2% with almost no change in the SD. In 6 of 8 cases, the Skintac adhesive produced better CNR values than the other 2 agents. Background mean and SD values show that Skintac had consistently low SD values while maintaining high background mean levels. However, the difference in CNR values between Got2b Glued and Skintac was found to be relatively small (<10% in all cases except 1). Furthermore, in terms of practicality, Skintac is not as viable as the next best agent, Got2b Glued; Skintac requires rigorous alcohol cleanup, whereas Got2b Glued can be removed easily with soap and water.

Therefore, we decided that the Got2b Glued adhesive hair spray was best for our application. In all cases, CNR values for Got2b Glued were degraded by no more than 20% compared with pure water. Got2b Glued preserved image quality, was empirically found to be a close second best for adhesively coupling the breast to the paddle, and was easy to remove and clean up.

Figure 7. Correlation maintained over time for the most suitable coupling agent for a stationary scan. The value largely stays above 0.8. The drop in correlation for frame 13 is likely to be due to patient motion.

Figure 8. Contrast-to-noise ratio values for both anechoic and –9-dB targets at depths of 2.5 and 4 cm for each coupling medium, where the ROI size is 55 square pixels. The largest (magnitude) value of –4.44 was obtained at the 4-cm depth for the anechoic target when water was used as the coupling medium in the absence of a TPX plate.
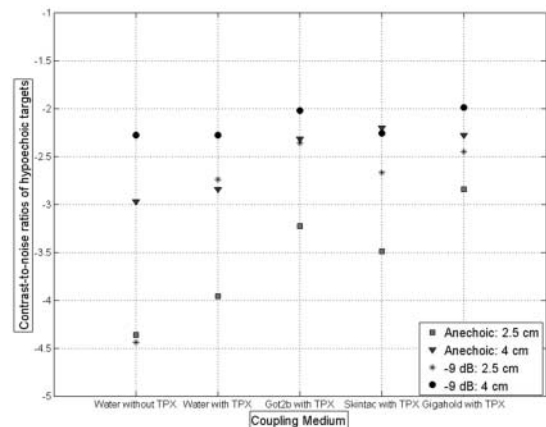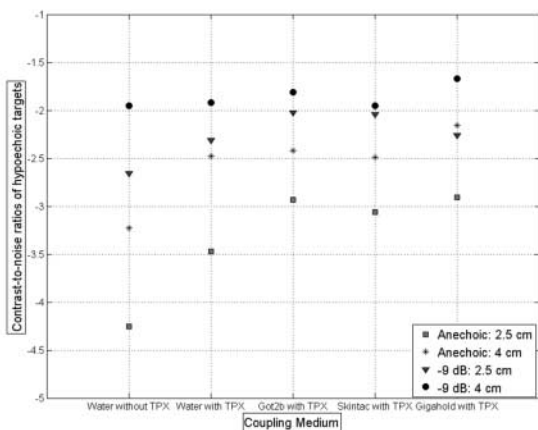
Figure 9. Contrast-to-noise ratio values for both anechoic and –9-dB targets at depths of 2.5 and 4 cm for each coupling medium, where the ROI size is 130 square pixels. The largest (magnitude) value of –4.25 was obtained at the 2.5-cm depth for the anechoic target when water was used as the coupling medium in the absence of a TPX plate.

Ten pure and 4 compound substances were tested for coupling the transducer to the paddle in the LM view. LithoClear ultrasound gel maintains high viscosity at body temperature (37°C) and proved most effective for coupling the transducer to the paddle for LM views. It is also used to increase the area of coverage by filling in the gap between the paddle and the outer edge of the breast. As of September 2006, 73 patients

Figure 10. Background mean and RMS noise values at depths of 2.5 and 4 cm for each coupling medium, where the ROI size is 55 square pixels. The highest mean level of 77.37 was obtained at the 2.5-cm depth when water was used as the coupling medium in the absence of a TPX plate. The lowest noise level of 14 was obtained at the 2.5-cm depth when water was used as the coupling medium in the presence of a TPX plate.
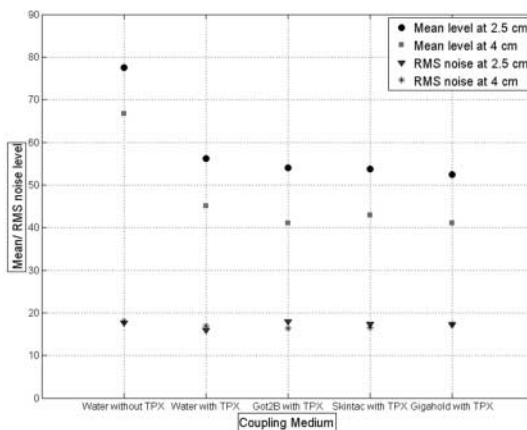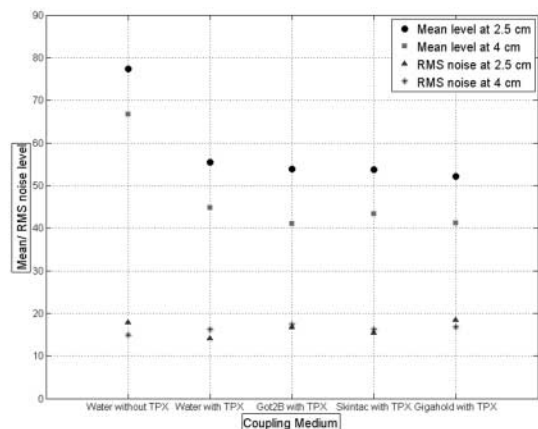

Figure 11. Background mean and RMS noise values at depths of 2.5 and 4 cm for each coupling medium, where the ROI size is 130 square pixels. The highest mean level of 77.53 was obtained at the 2.5-cm depth when water was used as the coupling medium in the absence of a TPX plate. The lowest noise level of 15.96 was obtained at the 2.5-cm depth when water was used as the coupling medium in the presence of a TPX plate.

have been imaged in CC and LM views of the affected breast with the experimentally superior coupling agents.

Motion Analysis
Patient motion artifact analysis carried out in both the B-mode and IQ mode proved that shallow patient breathing and breath holding were not harmful to image quality, whereas speech and sudden breathing produced unacceptable artifacts. The significant difference that was

Figure 12. Averages and SDs of the minimum correlation values observed for the left breasts of 6 patients in the following situations: breath holding, hold and release, shallow breathing, and talking (repetition of a single phrase).
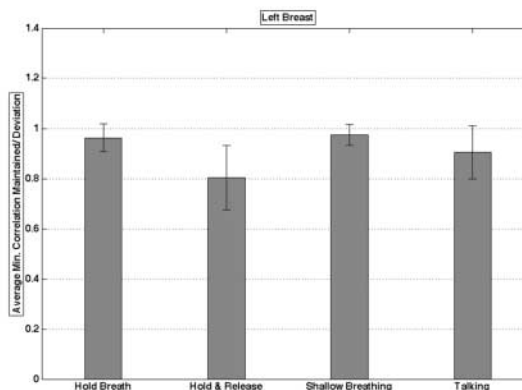
Figure 13. Averages and SDs of the minimum correlation values observed for the right breasts of 6 patients in the following situations: breath holding, hold and release, shallow breathing, and talking (repetition of a single phrase).
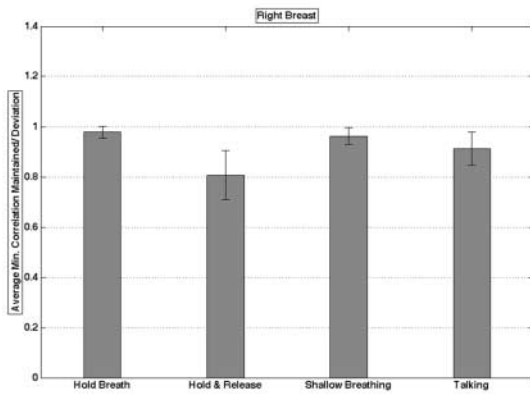
observed in the B-mode breath-holding data for the left and right breasts may have been caused by cardiac asymmetry; that is, when the patient held her breath, the heart pulsed more strongly because of the baroreceptor reflex. Hence, breath holding caused more decorrelation for the left breast. Such a difference between the images of the right and left breasts was not observed with shallow breathing.

The region-wise split for all motion conditions indicated that decorrelation was consistently (95% of the time) greatest toward the chest wall. This was expected because the motion of the chest wall causes a decorrelation when the patient is breathing or talking. Overall, because patient scans can be more than 1 minute long, shallow breathing is a more feasible option than breath holding.

By aiding the stabilization of the compressed breast, we succeeded in minimizing technical difficulties in image splicing and registration caused by slippage of the breast.

Conclusions

Limitations of automated ultrasound scanning on a multimodality breast imaging system have been addressed by developing methods to couple the transducer and breast to the compression paddle, as well as methods to fill in peripheral

Table 3. Averages and SDs for the 4 Motion Artifacts Analyzed for the Left and Right Breasts

Artifact	Mean		SD	
	Left Breast	Right Breast	Left Breast	Right Breast
Breath holding	0.963	0.056	0.979	0.023
Deep breath and release	0.805	0.128	0.807	0.098
Shallow breathing	0.974	0.042	0.962	0.034
Talking	0.906	0.106	0.912	0.066

Figure 14. A, Single slice of a spliced gray scale image volume from a recent patient with multiple cysts in the left breast. **B**, Same image slice. The vertical line indicates the joint between the adjacent scans.
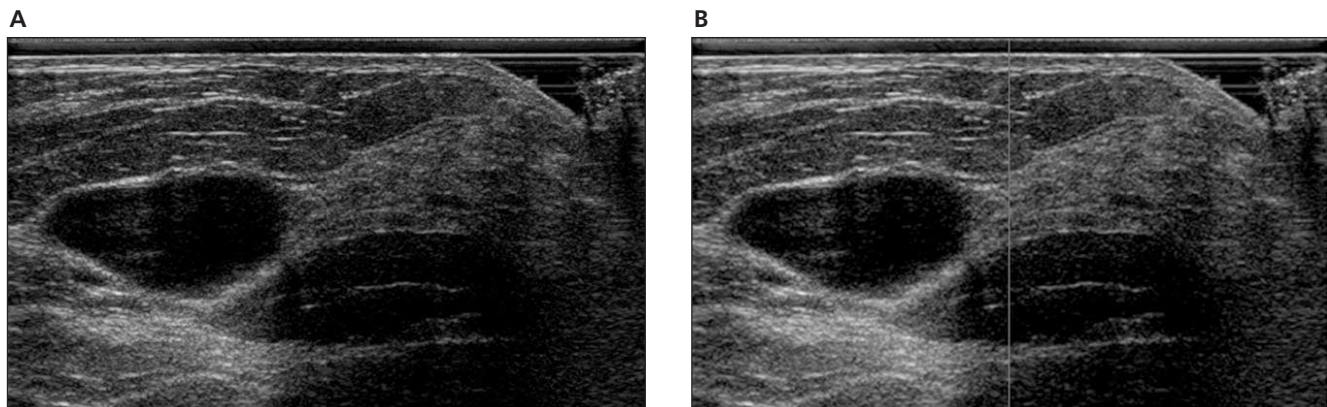
A

B

gaps, minimize patient motion, and register and reconstruct multisweep ultrasound image volumes after clinical acquisition. The ultrasound techniques described and evaluated in this study yielded ultrasound volumes that provided good comparisons with x-ray attenuation properties of the tissues as viewed in the high-speed, wide-angle, and low-dose x-ray tomosynthesis images. This direct comparison should improve visual and computer-assisted diagnosis.

References

1. LeCarpentier GL, Tridandapani PB, Fowlkes JB, Roubidoux MA, Moskalik AP, Carson PL. Utility of 3D ultrasound in the discrimination and detection of breast cancer. RSNA Electron J 1999; 3. Available at: http://ej.rsna.org/ej3/0103-99.fin/titlepage.html.

2. Kapur A, Carson PL, Eberhard J, et al. Combination of digital mammography with semi-automated 3D breast ultrasound. Technol Cancer Res Treat 2004; 3:325–334.

3. Carson PL, LeCarpentier GL, Roubidoux MA, Erkamp RQ, Fowlkes JB, Goodsitt MM. Physics and technology of ultrasound breast imaging including automated 3D. In: Karellas A, Giger ML (eds). 2004 Syllabus, Advances in Breast Imaging: Physics, Technology, and Clinical Applications. RSNA Categorical Course in Diagnostic Radiology Physics. Oak Brook, IL: Radiological Society of North America, 2004:223–232.

4. Booi RC, Krücker JF, Goodsitt MM, et al. Evaluating thin compression paddles for mammographically compatible ultrasound. Ultrasound Med Biol 2007; 33:472–482.

5. Sahiner B, Chan HP, Roubidoux MA, et al. Computer-aided diagnosis of malignant and benign breast masses in 3D ultrasound volumes: effect on radiologists' accuracy. Radiology 2007; 242:716–724.

6. Chan HP, Wei J, Sahiner B, et al. Computer-aided detection system for breast masses on digital tomosynthesis mammograms: preliminary experience. Radiology 2005; 237:1075–1080.

7. Eberhard JW, Staudinger P, Smolenski J, Ding J, Schmitz A, McCoy J, et al. A high-speed large-angle mammography tomosynthesis system. In: Physics of Medical Imaging: Proceedings of the SPIE Symposium on Medical Imaging. Bellingham, WA: SPIE; 2006:61420C_1–11.

8. van Wijk MC, Thijssen JM. Performance testing of medical ultrasound equipment: fundamental vs harmonic mode. Ultrasonics 2002; 40:585–591.

9. Kim B, Boes JL, Frey KA, Meyer CR. Mutual information for automated unwarping of rat brain autoradiographs. Neuroimage 1997; 5:31–40.

10. Krücker JF, Meyer CR, LeCarpentier GL, Fowlkes JB, Carson PL. 3D spatial compounding of ultrasound images using image-based, nonrigid registration. Ultrasound Med Biol 2000; 26:1475–1488.

11. Stacey-Clear A, McCarthy KA, Hall DA, et al. Mammographically detected breast cancer: location in women under 50 years old. Radiology 1993; 186:677–680.